Successive Impulsive Noise Suppression in OFDM

Anıl Mengi and A. J. Han Vinck
Institute for Experimental Mathematics
Duisburg-Essen University
Ellernstr. 29, D-45326, Essen
Germany
Email: {mengi;vinck}@iem.uni-due.de

***Abstract*—We consider orthogonal frequency division multiplexing (OFDM) for high data rate narrowband power line communication (PLC) in the frequency bands up to 500 kHz. In narrowband PLC, the performance is strongly influenced by the impulsive noise with very large amplitudes with short durations. Simple iterative impulsive noise suppression algorithms can effectively improve the error rate performance in OFDM systems. However, the convergence speed depends on the number of subcarriers, N. For $N \leq 256$, the algorithms converge slowly or not even at all. In this paper, we extend the iterative receiver design to enable a fast convergence for $N > 64$ and to improve the error rate performance for $N \leq 64$. These extensions include 1) a clipping and nulling technique at the input of the iterative algorithm 2) a novel low complexity syndrome decoder which uses the redundancy that is transmitted for synchronization or other purposes. Simulation results are provided to show the improvement in error rate.**

I. Introduction

Orthogonal frequency division multiplexing (OFDM) has been considered as a modulation scheme in high data rate (up to 1 Mbps) narrowband (9-500 kHz) power line communication (PLC) modems, see [1] and [2]. Impulsive noise with very large amplitudes with short (typically a few microseconds to milliseconds) durations is one of the main disturbances influencing the system performance, see [3]. The reason for this is that the discrete Fourier transform (DFT) at the OFDM receiver spreads the impulse energy over a portion of information symbols. This spreading was interpreted such that OFDM has been considered to be robust against the impulsive noise [4]. However, it was shown in [5] that impulsive noise leads to an enormous loss in the capacity, as well as in the error rate performance. Simple iterative impulsive noise suppression algorithms can improve the performance by exploiting the noise structure in the time and frequency domain, see [5] and [6]. In these algorithms, the number of subcarriers, N, plays an important role. For large $N > 256$, the convergence speed is fast, whereas, for $N \leq 256$, the algorithms converge slowly or not even at all. This is mainly due to the Gaussian approximation used in the algorithms for the distribution of the transformed random variables after DFT or inverse DFT (IDFT). As N increases, the approximation becomes more accurate.

The iterative algorithm as given in [5] is discussed in this paper. We first show that using a clipping and nulling technique at the input of the algorithm significantly improves the error rate performance, and it enables a fast convergence for $N > 64$. Furthermore, we extend the iterative algorithm with a low complexity syndrome decoder that uses pilot tones or zeros that are appended to the information for different purposes, such as synchronization. The decoder applies a successive impulsive noise error decoding instead of decoding all errors jointly. This approach has the advantage that the non-consecutive zeros or pilot tones can also be used in the decoding.

This paper is organized as follows. In section II, we present the impulsive noise channel model, and it is followed by the iterative impulsive noise suppression algorithm in Section III. The clipping and nulling technique is discussed in Section IV. Section V presents the extension of the iterative algorithm by a simple syndrome decoder. Finally, a conclusion is given in Section VI.

II. OFDM and impulsive Noise Channel Model

We assume in general that the input vector S to the OFDM modulator consists of $K \leq N$ information symbols with a symbol energy E_s and a zero vector of length $(N - K)$ appended to the information, i.e., $\mathbf{S} = (S_1, ..., S_K, 0, ..., 0)^T$. The transmitted OFDM symbol vector $\mathbf{s}$ with a signal variance $\sigma_s^2 = E_s$ can be expressed as $\mathbf{s} = \mathbf{W}^{-1}\mathbf{S}$, where $\mathbf{W}^{-1}$ is the IDFT matrix. Note that if the positions of the zeros are consecutive in a circular way, there is a similarity between the Reed-Solomon encoder and IDFT, see [7].

A two component mixture Gaussian noise model [8] is considered in this letter. At the time instant k, the time domain received signal r_k of the received vector $\mathbf{r} = (r_1, ..., r_N)^T$ can be expressed as $r_k = s_k + n_k$, where n_k is the additive non-Gaussian random variable of the noise vector $\mathbf{n} = (n_1, ..., n_N)^T$. The probability density function of the complex channel noise is given by

$$p_{n_k}(x) = \frac{(1-A)}{2\pi\sigma_0^2} \exp\left(\frac{-|x|^2}{2\sigma_0^2}\right) + \frac{A}{2\pi\sigma_1^2} \exp\left(\frac{-|x|^2}{2\sigma_1^2}\right), \quad (1)$$

where $\sigma_0^2 = \sigma_g^2$ with the additive Gaussian background noise variance σ_g^2 and $\sigma_1^2 = \sigma_i^2/A + \sigma_g^2$ with the variance of the Gaussian component of the impulsive noise, σ_i^2. The parameter A can be considered as the probability of impulse occurrence. For $A = 0.1$, the channel is highly impulsive, since 10% of the samples are corrupted by the impulsive noise. Moreover, we define $\Gamma = \sigma_s^2/\sigma_i^2$ as the ratio of the signal variance to the impulsive noise variance.

978-1-4244-5010-7/10/$26.00 ©2010 IEEE

III. Iterative Noise Suppression Algorithm

In this section, we review the iterative impulsive noise suppression algorithm as given in [5]. The block diagram of the receiver is depicted in Fig. 1. After transmission over the impulsive noise channel, maximum likelihood (ML) detection is applied on the transformed received vector $\mathbf{R}^{(0)} = \mathbf{W}\mathbf{r}$, where $\mathbf{W}$ is the DFT matrix. The detector maps the first K elements of $\mathbf{R}^{(0)}$ on a signal point in the QAM constellation, and the last $N-K$ elements are set to zero. The estimated input vector $\mathbf{S}^{(l)}$, $l \geq 0$, represents the result of the lth iteration in the iterative algorithm. $\mathbf{S}^{(l)}$ is then converted back into the time domain and subtracted from the received vector $\mathbf{r}$. The result, $\mathbf{n}^{(l)} = \mathbf{r} - \mathbf{s}^{(l)}$, is processed by the threshold detector to estimate the complex amplitudes at the positions of the impulsive noise, i.e.,

$$\widetilde{n}_k^{(l)} = \begin{cases} 0 & \text{for } |n_k^{(l)}| \leq T \\ n_k^{(l)} & \text{for } |n_k^{(l)}| > T, \end{cases} \tag{2}$$

where T represents the threshold calculated in [5]. The iterative process continues by subtracting the vector $\widetilde{\mathbf{n}}^{(l)}$ from $\mathbf{r}$. If $\mathbf{S}^{(l+1)} = \mathbf{S}^{(l)}$ for the first time, the iteration stops.

For $N \leq 256$, the impulse energy after DFT is not spread evenly over all the information symbols, and consequently, the reliability of the first noise estimation $\mathbf{n}^{(0)}$ is low. In this case, the algorithm's convergence behavior is also poor, see Fig. 4.

IV. Iterative Receiver with Clipping and Nulling

In this section, we consider two simple pre-processing techniques at the input of the iterative algorithm to increase the reliability of the first noise estimate $\mathbf{n}^{(0)}$. These are clipping and 'clipping and nulling'. The block diagram of the modified iterative receiver is depicted in Fig. 2.

A. Clipping

Clipping can be applied to the received vector r to reduce the power of the impulsive noise by limiting the maximum signal value. For the received signal r_k, the decision regions are given as

$$\widetilde{r}_k = \begin{cases} r_k & \text{for } |r_k| \leq T_{clip} \\ T_{clip} e^{j \arg r_k} & \text{for } |r_k| > T_{clip}, \end{cases}$$

where $T_{clip} = 2.2\sigma_s^2$ is the clipping threshold, see [9].

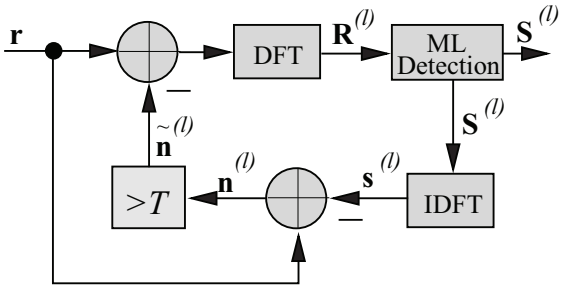

Fig. 1. Block diagram of the Haering's iterative receiver.

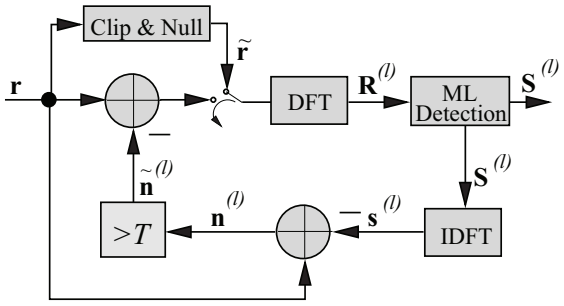

Fig. 2. Block diagram of the iterative receiver with clipping and nulling.

B. Clipping and Nulling

In [10], it has been shown that the 'clipping and nulling' technique significantly improves the performance of the conventional OFDM receiver. Since the mean value of the transmitted signal is zero, the amplitudes at the positions that are most likely hit by an impulse are set to zero. For the received signal r_k, the decision regions are given as

$$\widetilde{r}_k = \begin{cases} r_k & \text{for } |r_k| \leq T_{clip} \\ T_{clip} e^{j \arg r_k} & \text{for } T_{clip} < |r_k| \leq 1.4 T_{clip} \\ 0 & \text{for } |r_k| > 1.4 T_{clip}. \end{cases} \tag{3}$$

The pre-processed vector $\widetilde{\mathbf{r}} = (\widetilde{r}_1, ..., \widetilde{r}_N)^T$ is used for the first estimation of the input vector $\mathbf{S}^{(0)}$, see Section III. The input for the lth iteration is given by $\mathbf{r} - \widetilde{\mathbf{n}}^{(l)}$.

Fig. 3 shows the symbol error rate (SER) as a function of $E_s/2\sigma_g^2$ for the 64-OFDM transmission using 4-QAM over the impulsive noise channel model. The SER for the uncoded transmission over the AWGN channel is also plotted for comparison. For all curves, we consider no iteration, i.e. $l = 0$. We observe that using a clipping and nulling technique leads to a large improvement in the performance.

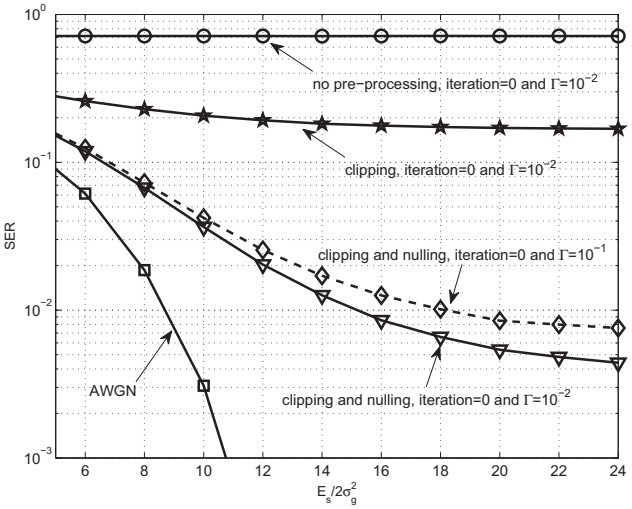

Fig. 3. SER of the 64-OFDM transmission over the impulsive noise channel with A=0.1 and $\Gamma = \sigma_s^2/\sigma_i^2$.

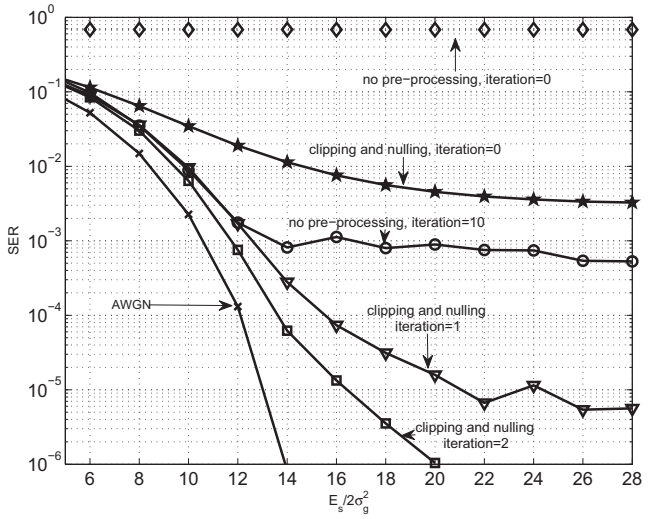

Fig. 4. SER of the iterative 128-OFDM transmission using 4-QAM over the impulsive noise channel with A=0.1 and $\Gamma = 10^{-2}$.

Fig. 4 shows the SER as a function of $E_s/2\sigma_g^2$ for the 128-OFDM transmission using iterative receiver. The performance results illustrate that SER decreases significantly using a low complexity clipping and nulling technique at the input of the iterative algorithm. The algorithm converges within two iterations, whereas no convergence is observed in the iterative algorithm described in Section III.

Fig. 5 shows the SER as a function of $E_s/2\sigma_g^2$ for the 256-OFDM transmission using iterative receiver. It can be observed that after only two iterations, the performance of the uncoded transmission over the AWGN channel is almost achieved.

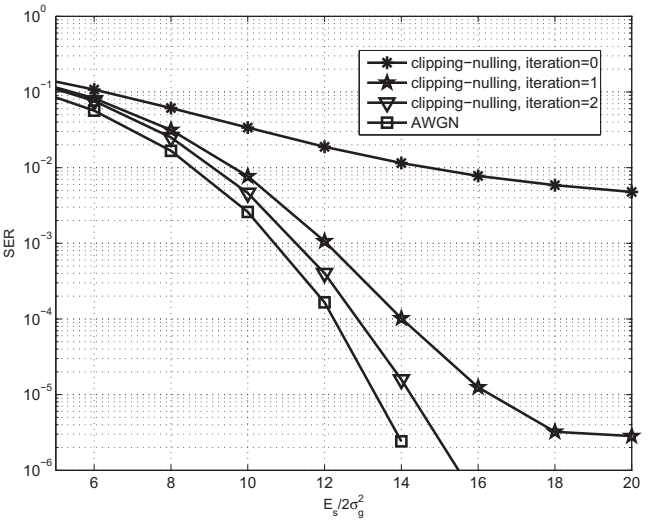

Fig. 5. SER of the iterative 256-OFDM transmission using 4-QAM over the impulsive noise channel with A=0.1 and $\Gamma = 10^{-2}$.

V. Iterative Receiver with 'Clipping and Nulling' and Syndrome Decoding

In this section we include a syndrome decoder in the receiver, located at the position as given in Fig. 6. At each iteration $l \geq 0$, $\mathbf{n}^{(l)}$ is processed by a modified threshold detector. Complex noise amplitudes at the positions where $|n_k^{(l)}| > T$ or $|r_k| > T_{clip}$ are passed through, whereas the values of other positions are set to zero. The syndrome decoder decodes the channel noise components one by one in descending order of magnitude of the obtained vector, $\widetilde{\mathbf{n}}^{(l)}$, see Fig. 7. Decoding of each channel noise component essentially involves four steps.

1) *Masking:* The component of $\widetilde{\mathbf{n}}^{(l)}$ with the largest magnitude is masked, that is, we set it to zero. The resulting vector, $\widetilde{\mathbf{n}}_{unmasked}$, is then subtracted from $\mathbf{r}$. In this step, we want to cancel the channel noise in $\mathbf{r}$, except for the noise at the position of the masked component.

2) *Syndrome former:* The last $N-K$ positions at the input of the OFDM modulator are set to zero. Hence, the syndrome vector $\mathbf{S}_{syn}$ can be calculated by an $(N-K)\times N$ matrix $\mathbf{H}^H$, the Hermitian transpose of the parity-check matrix $\mathbf{H}$, where $\mathbf{H}^H\mathbf{W}^{-1}\mathbf{S} = 0$. The vector $\mathbf{S}_{syn}$ depends only on the noise components, not on the transmitted OFDM symbol. Thus, $\mathbf{S}_{syn} = \mathbf{H}^H(\mathbf{r} - \widetilde{\mathbf{n}}_{unmasked}) = \mathbf{H}^H(\mathbf{n} - \widetilde{\mathbf{n}}_{unmasked})$.

3) *Decoding of the noise at the masked position:* We want to estimate the channel noise component, n_{masked}, at the position of the masked component of $\widetilde{\mathbf{n}}^{(l)}$. Given that position, the syndrome vector $\mathbf{S}_{syn}$ can be rewritten as

$$\mathbf{S}_{syn} = \mathbf{H}_{sub} n_{masked} + \mathbf{H}^H \mathbf{e}, \tag{4}$$

where $\mathbf{H}_{sub}$ is the $(N-K)\times 1$ sub-matrix of $\mathbf{H}^H$ containing its column at the position of the masked component. The contribution $\mathbf{H}^H\mathbf{e}$ follows from $(\mathbf{n} - \widetilde{\mathbf{n}}_{unmasked})$ at the positions of the unmasked components. By applying the Moore-Penrose pseudo-inverse [11] of $\mathbf{H}_{sub}$, a least square solution to Eq. (4)

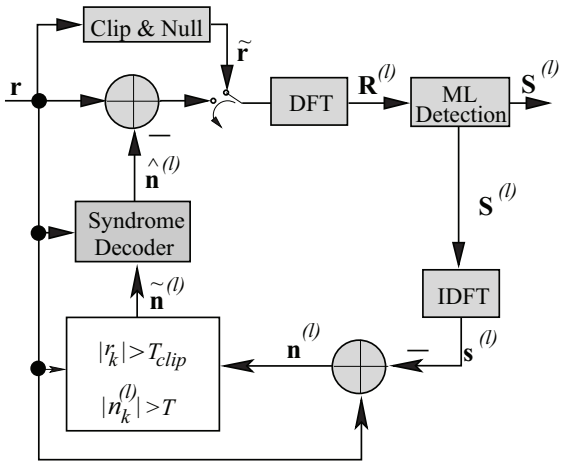

Fig. 6. Block diagram of the proposed iterative receiver

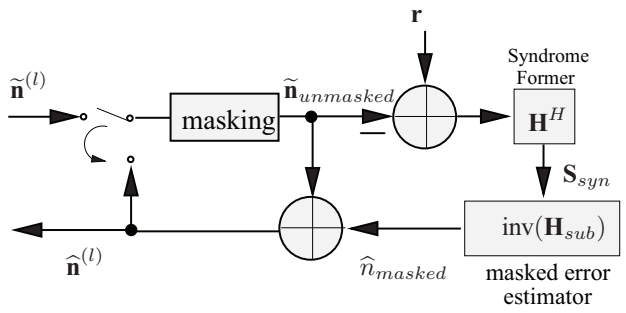

Fig. 7. Block diagram of the syndrome decoder

is given by

$$\begin{aligned}\widehat{n}_{masked} &= (\mathbf{H}_{sub}^H\mathbf{H}_{sub})^{-1}\mathbf{H}_{sub}^H\mathbf{S}_{syn} \\ &= n_{masked} + (\mathbf{H}_{sub}^H\mathbf{H}_{sub})^{-1}\mathbf{H}_{sub}^H\mathbf{H}^H\mathbf{e}. \quad (5)\end{aligned}$$

4) *Removing the decoded noise component:* The computed $\widehat{n}_{masked}$ is added to $\widetilde{\mathbf{n}}_{unmasked}$ at the position of the masked component. Then, in the result, the complex amplitude at the position of the next largest magnitude of $\widetilde{\mathbf{n}}^{(l)}$ is masked. It can be observed that the estimation error in Eq. (5), $(\widehat{n}_{masked} - n_{masked})$, propagates to the decoding of the next component. The covariance of the estimation error can be calculated as

$$\begin{aligned}\Phi_{syn} &= \mathrm{E}\{(\widehat{n}_{masked} - n_{masked})(\widehat{n}_{masked} - n_{masked})^H\} \\ &= N_e(\mathbf{H}_{sub}^H\mathbf{H}_{sub})^{-1}, \quad (6)\end{aligned}$$

where $N_e\mathbf{I}_N = \mathrm{E}\{\mathbf{e}\mathbf{e}^H\}$, N_e denotes the power of e and $\mathbf{I}_N$ is the identity matrix of size $N \times N$. In (6), small eigenvalues of $\mathbf{H}_{sub}^H\mathbf{H}_{sub}$ will lead to a large estimation error. Since $\mathbf{H}_{sub}$ has dimensions $(N-K)\times 1$, the factor, $(\mathbf{H}_{sub}^H\mathbf{H}_{sub})^{-1}$, can be calculated as $N/(N-K)$. Hence, an increase in $N-K$ leads to a better error rate performance of the receiver. Note that the Moore-Penrose pseudo-inverse of $\mathbf{H}_{sub}$ can be written as $N/(N-K)\mathbf{H}_{sub}^H$. In this case, the inverse of $\mathbf{H}_{sub}$ always exists independent from the position of zeros. Thus, decoding the noise components one by one has the advantage that the non-consecutive zeros and pilot tones can also be used in the decoding algorithm. An alternative approach is to decode up to $N-K$ noise components jointly. However, there are two main disadvantages. **(1)** Only consecutive redundant data can be used for syndrome decoding to ensure the existence of the inverse of $\mathbf{H}_{sub}$. **(2)** A large amplification factor can be expected.

At each iteration $l \geq 0$, the algorithm continues until all positions in $\widetilde{\mathbf{n}}^{(l)}$ are estimated. The output vector $\widehat{\mathbf{n}}^{(l)}$ contains the complex noise amplitudes of the lth iteration that are successively decoded by the syndrome decoding. The iteration process continues by subtracting the vector $\widehat{\mathbf{n}}^{(l)}$ from $\mathbf{r}$. The complexity of the syndrome decoding depends on the number of masked positions at each iteration. On the average, AN impulses occur during the transmission of one OFDM symbol. For small σ_g^2 , $A = 0.1$ and $N = 32$, it corresponds to a successive decoding of about 3 impulses on average.

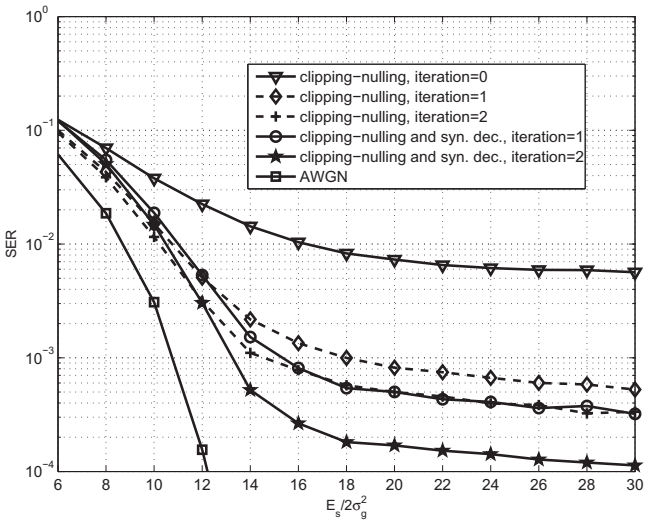

Fig. 8. SER of the iterative 32-OFDM transmission using 4-QAM over the impulsive noise channel with A=0.1 and $\Gamma = 10^{-2}$.

Fig. 8, Fig. 9 and Fig. 10 show the SER as a function of $E_s/2\sigma_g^2$ for the transmission over the highly impulsive channel model. We consider four zeros in 32-OFDM and eight in 64-OFDM, respectively. We observe in Fig. 8 that using syndrome decoding at the iterative receiver results in a lower SER beyond 12 dB. A large gain can be obtained after only two iterations. Since more iterations improve the results slightly, they are not shown in the figure. For $N = 64$, the performance gain due to the syndrome decoding is significant with decreasing σ_g^2, see Fig. 9 and Fig. 10. For $\Gamma = 10^{-2}$, the SER drops to 10^{-6} at 27 dB and for $\Gamma = 10^{-3}$ at 18 dB, respectively.

The parameters $\Gamma = \sigma_s^2/\sigma_i^2$, $(N-K)$ and A have an influence on the iterative receiver's performance. As σ_i^2 increases,

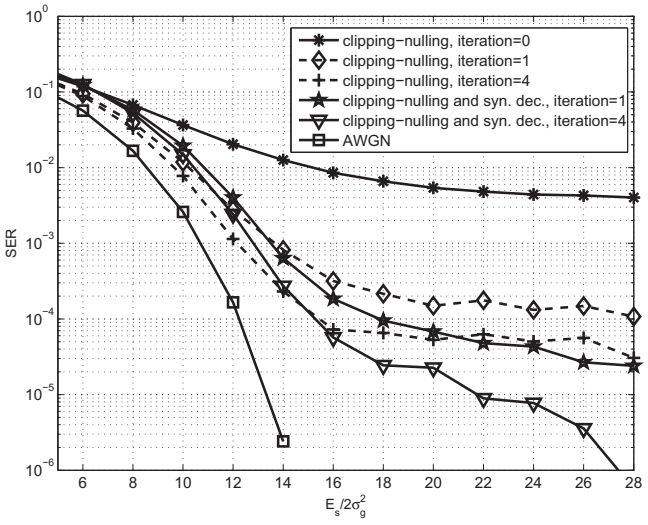

Fig. 9. SER of the iterative 64-OFDM transmission using 4-QAM over the impulsive noise channel with A=0.1 and $\Gamma = 10^{-2}$.

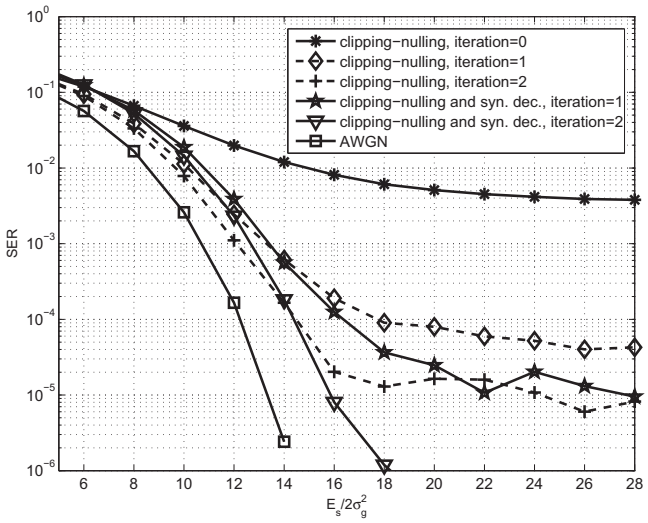

Fig. 10. SER of the iterative 64-OFDM transmission using 4-QAM over the impulsive noise channel with A=0.1 and $\Gamma = 10^{-3}$.

the impulsive noise magnitudes can be clearly distinguished by the threshold detector in the frequency domain. Hence, the SER of the iterative receiver also decreases, see Fig. 9 and Fig. 10. Increasing $(N - K)$ leads to a better SER performance since the amplification factor in (6) is decreasing. Thus, an additional gain can also be achieved by adding zeros to the information for the decoding of impulsive noise errors only. Finally, A determines the number of impulsive noise errors in an OFDM block.

VI. Conclusion

The performance of the iterative impulsive noise suppression algorithm depends on the number of subcarriers in OFDM. In this paper, we first show that applying the clipping and nulling technique at the front of the iterative algorithm decreases the SER significantly, and it leads to a fast convergence for $N > 64$. Furthermore, we demonstrate a novel syndrome decoding technique which uses the zeros or pilot tones that are transmitted for synchronization or other purposes. Instead of decoding all noise components jointly, a successive decoding is applied to achieve a low SER. This approach has the advantage that the non-consecutive zeros or pilot tones can also be used in the decoding algorithm.

References

[1] M. Deinzer, M. Stoeger, "Integrated PLC-modem based on OFDM," in *Proc. Int. Symp. Power Line Communications (ISPLC)*, Lancaster, UK, Apr. 1999, pp. 92-97.

[2] Maxim Integrated Products, "10kHz to 490kHz OFDM-based power line communication modem," in *Abridged Data Sheet*, 2008.

[3] O. G. Hooijen, "A channel model for the low-voltage power-line channel; measurement and simulation results," in *Proc. Int. Symp. Power Line Communications (ISPLC)*, Essen, Germany, Apr. 1997, pp. 51-56.

[4] J. Bingham, "Multicarrier modulation for data transmission: An idea whose time has come," *IEEE Commun. Mag.*, pp. 5-14, May 1990.

[5] J. Haering, A. J. H. Vinck, "OFDM transmission corrupted by impulsive noise," in *Proc. IEEE Int. Symp. Power Line Communications (ISPLC)*, Limerick, Ireland, Apr. 2000, pp. 9-14.

[6] S. V. Zhidkov, "Impulsive noise suppression in OFDM based communication systems," *IEEE Trans. on Consumer Electronics*, vol. 49, no. 4, pp. 944-948, Nov. 2003.

[7] J. K. Wolf, "Redundancy, the discrete Fourier transform, and impulse noise cancellation," *IEEE Trans. Commun.*, vol.COM-31, no. 3, pp. 458-461, Mar. 1983.

[8] M. Ghosh, "Analysis of the effect of impulsive noise on multicarrier and single carrier QAM systems," *IEEE Trans. Commun.*, vol. 44, No. 2, pp. 145-147, Feb. 1996.

[9] H. A. Suraweera, C. Chai, J. Shentu, J. Amstrong, "Analysis of impulse noise mitigation techniques for digital television systems," in *Proc. 8th Int. OFDM Workshop (InOWo'03)*, Hamburg, Germany, Sep. 2003, pp. 172-176.

[10] S. V. Zhidkov, "Analysis and comparison of several simple impulsive noise mitigation schemes for OFDM receivers," *IEEE Trans. Commun.*, vol. 56, no. 1, pp. 5-9, Jan. 2008.

[11] A. Ben-Israel, T. N. E. Greville, "*Generalized Inverses: Theory and Applications*." New York: Wiley, 1977.